Available online at www.sciencedirect.com
SCIENCE DIRECT®
Biochemical and Biophysical Research Communications 302 (2003) 101–108
BBRC
www.elsevier.com/locate/ybbrc

A HERG current sustains a cardiac-type action potential in neuroblastoma S cells

Massimo D'Amico,[a] Tiziana Biagiotti,[a] Lucrezia Fontana,[a] Rita Restano-Cassulini,[b] Nadia Lasagna,[a] Annarosa Arcangeli,[a] Enzo Wanke,[b] and Massimo Olivotto[a,*]

[a] *Department of Experimental Pathology and Oncology, University of Florence, Viale Morgagni 50, Florence 50134, Italy*
[b] *Department of Biotechnology and Biosciences, University of Milano Bicocca, Piazza delle Scienze 2, Milan 20126, Italy*

Received 21 January 2003

Abstract

From the adrenergic SH-SY5Y human neuroblastoma clone, we isolated a subclone (21S) endowed with a glial-oriented phenotype. At difference from the parental clone, 21S cells responded to depolarizing stimuli with overshooting action potentials, whose repolarization phase was composed of an initial rapid episode, followed by a long-lasting plateau and a slow return to the resting potential (V_{REST}). The action potential depolarization phase was sustained by a TTX-sensitive Na^+ current, while the first repolarizing episode was produced by the scanty delayed rectifier potassium current (I_{KDR}) expressed in 21S cells. The bulk of repolarization, including the after-hyperpolarization, was sustained by the human eag related (HERG) potassium current (I_{HERG}) that also governs V_{REST} in 21S cells. This double role of I_{HERG}, together with the poor expression of I_{KDRs}, represents a novel finding in electrophysiology, as well as gives a clue to identify a new excitable element of the complex cellular population of neuroblastoma.

Keywords: Neuroblastoma; Substrate adherent-cells (S-cells); HERG channels; Resting potential and action potential

HERG (human *eag* related) potassium channels [1] govern the resting potential (V_{REST}) in various cell types, which are devoid of classical inward rectifier (IRK) channels. Hence, the depolarization of V_{REST} through a diminution of the HERG current (I_{HERG}) correlates with apparently distant cellular functions, such as muscle contraction, O_2 sensing, and hormone secretion [2]. Moreover, I_{HERG} is expressed during immature stages of neuronal differentiation [3], and in tumors of varying histogeneses [4]. HERG channels are characterized by the following properties: (i) they can transit to and from an open (activated) or closed (deactivated) conformation (deactivation) with a transition governed by one gate, or from an inactivated to a deinactivated conformation (inactivation removal) with a transition governed by another gate [2,5]. Only when they are simultaneously open and deinactivated, they conduct the current; (ii) at negative holding potentials they are closed and deinactivated, while at positive potentials they are both inactivated and open; (iii) inactivation is faster than activation and recovery from inactivation (deinactivation) is considerably faster than deactivation. Therefore, unique among the voltage-gated potassium currents, I_{HERG} exhibits a strong inward rectification, so that a strong depolarization elicits a small current transient, followed by a small steady-state outward current.

Altogether, these biophysical features cause that, when V_{REST} is governed by I_{HERG} [9], it cannot be more negative than −40/−50 mV, due to the decrease of the current at membrane potentials more negative than −50 mV [3–5]. More negative values (−60/−80 mV) are attained in muscle cells and neurons by classical IRK channels, whose small outward current shifts V_{REST} towards the potassium equilibrium potential (E_K). Consistently, I_{HERG} substitutes the IRK current in the governing of V_{REST} in tumors or immature excitable tissues, which are invariably characterized by depolarized V_{REST} values [3–5,9].

* Corresponding author. Fax: +39-055-428-2333.
E-mail address: olivotto@unifi.it (M. Olivotto).

0006-291X/03/$ - see front matter © 2003 Elsevier Science (USA). All rights reserved.
doi:10.1016/S0006-291X(03)00121-9

By its nature, I_{HERG} is also apt to mediate the spike frequency adaptation [6] in neuronal-type cells, as well as to contribute to the ionic mechanisms underlying repolarization of the action potential in ventricular myocytes [2]. As repolarization proceeds, a transient increase in I_{HERG} occurs due to fast recovery from inactivation and slow deactivation, and cooperates with I_{Ks} and the classical cardiac rectifier current (I_{K1}) to repolarize the action potential and restore V_{REST} [2–5]. So far, however, a dominant role of I_{HERG} in the nervous action potential repolarization has not been described.

We show here that such a dominant role is played by I_{HERG} in the repolarization phase of action potentials elicited in a subclone (21S) isolated from the SH-SY5Y adrenergic clone of human neuroblastoma. Although SH-SY5Y cells are adrenergic neuronal-type cells, 21S cells displayed the glial phenotype previously identified in a cellular component of the multifaceted cell population of human neuroblastomas, the so called substrate-adherent (S) cells [7,14,20]; these ones have been regarded as possible sources of chemotherapy- and radiotherapy-resistant clones arising in the course of neuroblastoma progression in vivo [8]. 21S cells turned out to be endowed with an ion channel apparatus essentially composed of sodium and HERG channels, and responded to depolarizing stimuli with cardiac-type action potentials, characterized by a long-lasting plateau and a slow return to V_{REST}. These features evidence new aspects of HERG cellular functions and provide useful electrophysiological markers for an important element of the cellular population of neuroblastomas.

Materials and methods

Cell culture and cloning. SH-SY5Y cells (henceforth abbreviated as SY5Y) were maintained in RPMI 1640 medium (Euroclone) supplemented with 10% foetal calf serum (FCS) (Hyclone) in air containing 5% CO_2, as previously described [9]. The 21S clone, obtained by limiting dilution of SY5Y cells, initially displayed the typical S cell phenotype, but after varying times spent in culture, it generated an increasing number of neural-type cells that were routinely eliminated by vigorous washing of the cultures with PBS [8].

Immunofluorescence. Cells were seeded onto 18-mm glass coverslips and cultured as above in 35-mm plastic Petri dishes (Corning-Costar). After 48 h, cell cultures were fixed with 3.7% paraformaldehyde in PBS and stained with primary antibody to vimentin (1:2000; Sigma) and, subsequently, with αCy3-conjugated mouse secondary antibody (1:200; Chemicon).

Western blotting. SY5Y and 21S cells were lysed with RIPA buffer pH 7.0 (Na_2HPO_4 1 mM, NaCl 150 mM, Na_2EDTA 2 mM, 1% Na deoxycholate, 0,1% SDS, 0,1% Nonidet, 1 mM PMSF, 0.1 U/ml aprotinin, and 4 μg/ml pepstatin). Proteins were separated on a 10% SDS–polyacrylamide gel and electrotransferred onto a PVDF membrane (0.35 μm pore size, Amersham Pharmacia). The membrane was incubated overnight at 4 °C with primary antibodies: vimentin 1:1000, GFAP 1:1500, and NF-68 1:500 (Sigma). The next day, the membrane was incubated with peroxidase-conjugated secondary antibody (Sigma).

Patch-clamp recordings. Cells were seeded on 35 mm Petri dishes and traces were recorded with the amplifier Axopatch 200 A (Axon Instruments), using the whole cell configuration [10]. Measurements of the membrane potential and currents were performed in current-clamp ($I = 0$ mode) or voltage clamp, respectively. Pipettes' resistances were between 3 and 5 MΩ (borosilicate glass, Harvard Apparatus). Gigaseal resistances were in the range 10–20 G. Input resistances of the cells were in the range 2–6 GΩ. Whole cell currents were filtered at 1–3 kHz. For data acquisition and analysis, the pClamp and Axoscope software (Axon Instruments, Foster City, CA) and Origin (Microcal Software, Northampton, MA) were routinely used. For a precise measurement of the current gating parameters, pipette and cell capacitance and the series resistance (up to 70–80%) were carefully compensated before each voltage clamp protocol run.

I_{HERG} activation and inactivation curves were measured according to Faravelli et al. [11] and Smith et al. [12]. Perforated patch recordings were obtained using amphotericin according to Rae et al. [13].

Solutions: The extracellular solution with low potassium (low K_o solution) contained (mM): NaCl 130, KCl 5, $CaCl_2$ 2, $MgCl_2$ 2, Hepes–NaOH 10, and glucose 5, pH 7.4. The extracellular solution with high potassium (high K_o solution) contained (mM): NaCl 95, KCl 40, $CaCl_2$ 2, $MgCl_2$ 2, Hepes–NaOH 10, and glucose 5, pH 7.4. The extracellular solution for Ca^{2+} currents contained (mM): NaCl 120, $BaCl_2$ 10, $MgCl_2$ 2, glucose 5, Hepes 10, and TTX 3 μM, pH 7.4. The standard pipette solution at $[Ca^{2+}] = 10^{-7}$ M contained (mM): K^+ aspartate 130, NaCl 10, $MgCl_2$ 2, $CaCl_2$ 2, EGTA–KOH 10, and Hepes–KOH 10, pH 7.4. For perforated patch experiments the pipette solution contained (mM): K^+ aspartate 140, NaCl 10, $MgCl_2$ 2, Hepes–KOH 10, and amphotericin B 150 μg/ml.

Results and discussion

While the parental SY5Y clone was thoroughly characterized in previous studies [3,4,7–9,15], 21S cells were here analyzed for the following aspects.

Phenotype

21S cells displayed the epithelial-like morphology characteristic of S cells, appearing large, flattened, and highly substrate-adherent (Fig. 1A), and profoundly differing from the parental SY5Y cells, characterized by an abortive neuronal phenotype. In keeping with their S-type morphology, 21S cells were strongly positive to anti-vimentin antibodies (Fig. 1B) [7,14] and, compared to parental cells, they expressed higher levels of vimentin and GFAP, and lower levels of 68 neurofilaments (Fig. 1C).

On the whole, the 21S subclone apparently lacks the neuronal phenotype, while displaying that of S cells committed to an astrocytic differentiation lineage [7,14].

V_{REST}

21S cells turned out to have a V_{REST} averaging at −42 mV (Table 1); in a conspicuous number of cells, we measured values of −50/−60 mV, never recorded in N-type cells.

The evocated electrical activity

Toselli et al. [15] demonstrated that the electrophysiological asset of neuronal-type SY5Y cells is substan-

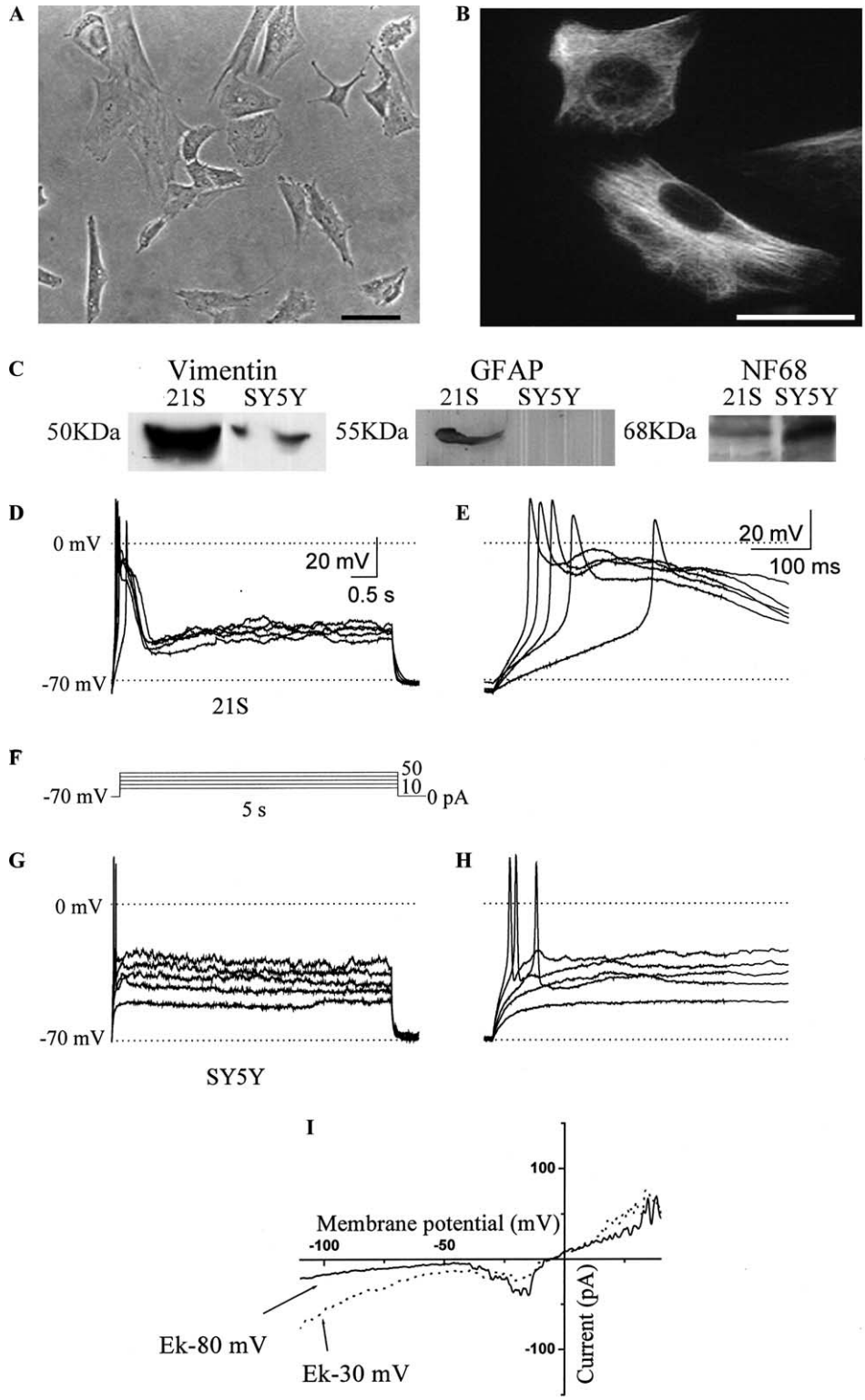

Fig. 1. (A) 21S cells in standard culture (bar = 75 μm); (B) 21S cells decorated with anti-vimentin antibodies. This image was obtained by immunofluorescence, as reported in Materials and methods (bar = 50 μm); (C) different expression of cellular markers in 21S and in the parental SY5Y cells. Western blotting experiments, using antibodies against: vimentin, GFAP and Neurofilaments-68; (D,G) the action potential shape of 21S cells (D) as compared to parental SY5Y cells (G). Patch-clamp recordings in whole cell configuration and in current-clamp. Cells were injected with 5 s lasting-current pulses of 10–50 pA (protocol in F); (E,H) traces obtained from (D) and (G), respectively, after rescaling; (I) the electrophysiological profile of 21S cells. A typical 21S cell was patched in whole cell configuration in voltage clamp; currents were elicited by a 360 ms long ramp command ranging from −120 to +60 mV. Measurements were carried out either in the standard, low K^+, external solution ($[K^+]_o = 5$ mM; $E_K = -80$ mV), or in the high K^+ solution ($[K^+]_o = 40$ mM; $E_K = -30$ mV).

Table 1
Biophysical parameters of ion currents expressed in 21S cells

Capacitance (pF)	12.45 ± 0.40 (179)
V_{REST} (mV)	−42 ± 0.4 (79)
I_{Na^+} (pA)[a]	−1016.6 ± 85.4 (25)
δI_{Na^+} (pA/pF)	70.6 ± 6.7 (25)
$V^g_{1/2\ Na^+}$ (mV)	−18.2 ± 0.8 (25)
$dx^g_{Na^+}$ (mV)	5.6 ± 0.34 (25)
$V^h_{1/2\ Na^+}$ (mV)	−53.8 ± 1.14 (26)
$dx^h_{Na^+}$ (mV)	8.25 ± 0.25 (26)
I_{HERG} (pA)	1209 ± 83 (164)
δI_{HERG} (pA/pF)	101.64 ± 6.6 (151)
$V^g_{1/2\ HERG}$ (mV)	−47.8 ± 1.1 (13)
dx^g_{HERG} (mV)	4.9 ± 0.3 (13)
$V^h_{1/2\ HERG}$ (mV)	−72 ± 3.0 (10)
dx^h_{HERG} (mV)	25.5 ± 1.0 (10)
I_{KDR} (pA)	243.1 ± 13.04 (179)
δI_{KDR} (pA/pF)	23.2 ± 1.7 (179)

Values are means ± SEM of a number of cells indicated in parentheses.

[a] The sodium currents were measured either in the presence or in the absence of 2 μM TTX and subtracting the TTX traces (TTX-sensitive currents). *Abbreviations:* V_{REST}, resting potential; I_{HERG}, maximal peak of HERG current; δI_{HERG}, HERG current density; I_{KDR}, maximal peak KDR current; δI_{KDR}, KDR current density; I_{Na}, maximal peak of Na^+ current; δI_{Na}, Na^+ current density; $V^g_{1/2}$, $V_{1/2}$ of activation curve; dx^g, slope of activation curve; $V^h_{1/2}$, $V_{1/2}$ of inactivation curve; dx^h, slope of inactivation curve.

tially unable to generate overshooting action potentials, mainly due to a scanty I_{Na} density and unsuitable gating properties of Na^+ and K^+ channels. This difficulty was confirmed under our conditions; in fact, intracellular injection of rectangular depolarizing current from a hyperpolarized membrane potential (−60, −70 mV; see protocol in Fig. 1F), in most cases, failed to elicit regenerative voltage responses (not shown). Surprisingly, when this protocol was applied to 21S cells, we found that 60% of them responded with an overshooting action potential (Figs. 1D and E). This potential displayed a typical overshoot and a repolarization phase, composed of two distinct episodes: (1) a rapid initial voltage increase that extinguished shortly; (2) a slow long-lasting depolarizing plateau that mimicked that of the cardiomyocyte action potential. To our knowledge, this cardiac-type feature was not described for action potentials elicited in neuroblastoma cells, either treated with retinoic acid [15,16], or in the rare excitable undifferentiated cells; in the latter, in fact, this plateau was absent and the repolarization phase was a monotonous and much faster process (Figs. 1G and H).

The electrophysiological profile

As a first clue to identify the major currents expressed in 21S cells, we explored the I/V plot reported in Fig. 1I, recorded in low or in high potassium external solutions. This plot was characterized by: (i) no trace of IRK current; (ii) an evident inward current in the voltage range of I_{HERG}; (iii) a sizeable inward current in the voltage range (about −20 mV) of I_{Na} activation; and (iv) a scanty (often negligible) outward current in the voltage range eliciting I_{KDR}. Such a low expression of this current turned out to be a constant marker of 21S cell electrophysiological phenotype, identifying these cells within the multifaceted neuroblastoma cell population.

The ionic currents

A detailed analysis of the currents identified in 21S cells was performed as reported below.

I_{Na}. When applied to S cells, the protocol reported in 2C elicited inward Na^+ currents, characterized by rapid activation and inactivation kinetics (Fig. 2A) and abolished by 2 μM TTX (not shown). Only very weak outward I_{KDR} was elicited. The average values of I_{Na} and I_{KDR}, and the respective densities (pA/pF) are reported in Table 1. The normalized plot of sodium peak current vs V_M is shown in Fig. 2B. A further characterization of the TTX-sensitive I_{Na} was performed by analyzing the voltage-dependence of the steady-state activation (g(V)) and inactivation (h(V)) (Fig. 2D and Table 1) that turned out to be very similar to those reported for astrocytoma cells [17].

I_{HERG}. When applying the protocols reported in Figs. 2H and I, typical HERG tail currents were elicited in 21S cells (Figs. 2E and F); these currents were totally abolished by the HERG specific inhibitor WAY (2 μM) Fig. 2G).These records also reveal the lack of IRK current in 21S cells. Fig. 2J shows the voltage-dependence of I_{HERG} steady-state activation, g(V), and inactivation, h(V), calculated by best fitting with Boltzmann curves the data obtained using the protocols reported in Figs. 2H and I, respectively. The calculated steady-state conductance (g(V)*h(V)) peaks at about −40 mV, a value close to the average V_{REST} of 21S cells (see Table 1), supporting that this potential is governed by HERG channels in S cells, as it is in SY5Y cells [13] (but see below).

I_{KDR}. This current, sometimes barely detectable, was constantly expressed at low density in 21S cells (Table 1); in any case, it turned out to be electrophysiologically and pharmacologically similar to that described in SY5Y cells by Tosetti et al. [16], except for a +10 mV shift of the activation curve, which makes the I_{KDR} contribution even more irrelevant to the regulation of V_{REST} in 21S cells.

hEag current. This current was sizeable only in 28% and scarcely detectable in 72% of tested 21S cells, with an average value of 6.76 ± 2.4 pA/pF (means ± SEM; $n = 32$). This value is at least 10-fold lower than that reported by Meyer and Heinemann [18] and practically negligible as compared to I_{HERG}.

Ca^{2+} currents. These currents were never detectable in the tested 21S cells ($n = 30$).

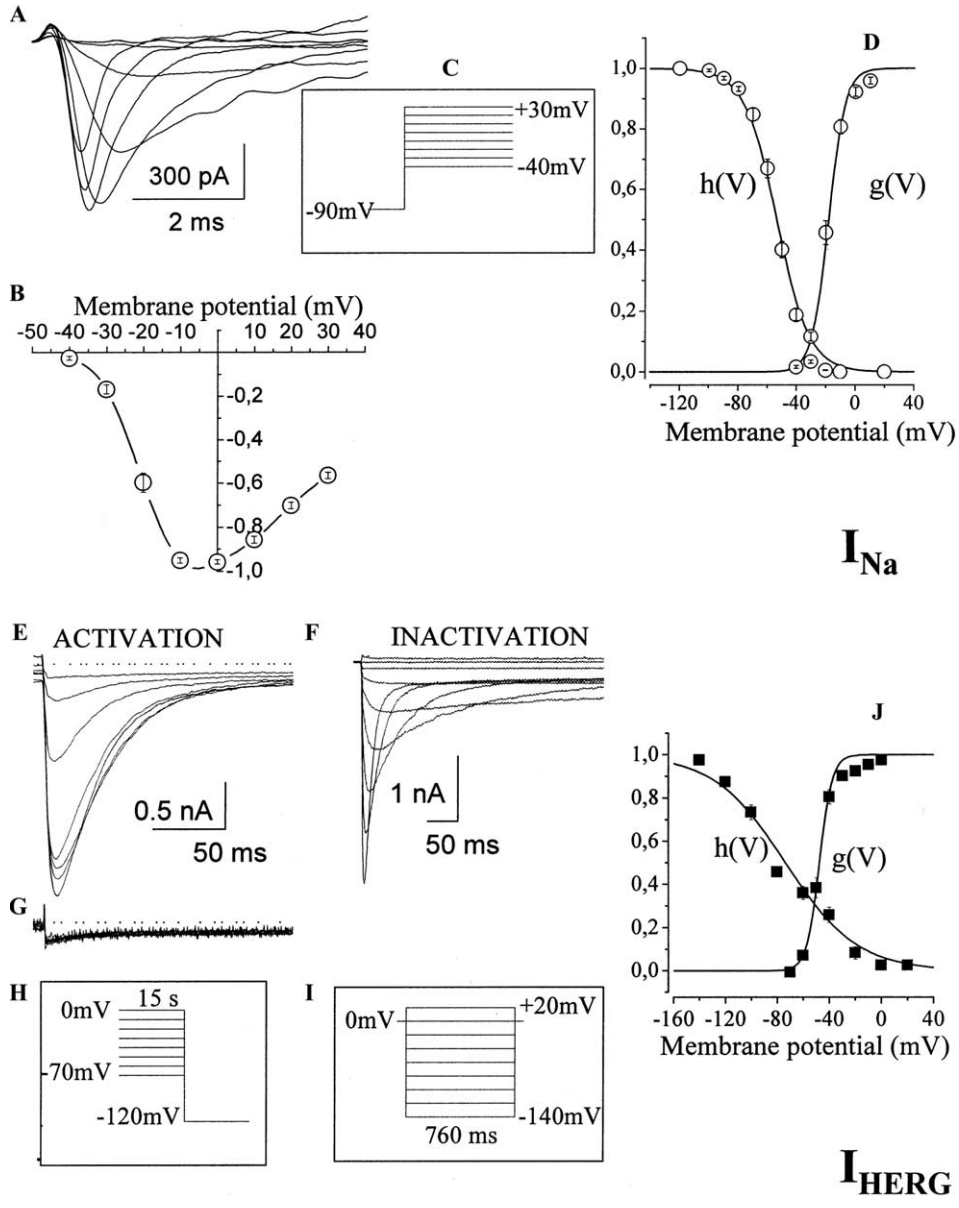

Fig. 2. Ion currents expressed in 21S cells and effects of inhibitors. (A) I_{Na} elicited by the protocol reported in (C); (B) the I/V plot obtained normalizing the currents recorded in A as I/I_{MAX}. Symbols represent means ± SEM of currents recorded in 11 cells; (D) voltage-dependent activation (g(V)) and inactivation (h(V)) of TTX-sensitive currents (2 μM TTX). Symbols represent means ± SEM of currents recorded in 11 cells; (E,F) I_{HERG} elicited in 40 mM external potassium ($E_K = -30$ mV) by the protocols reported in (H) (activation) and (I) (inactivation), respectively; the blockade of I_{HERG} by 2 μM WAY (G); (J) the voltage-dependence of I_{HERG} steady-state activation (g(V)) and inactivation (h(V)). Symbols represent means ± SEM of currents recorded in 25 cells.

The effects of various currents inhibitors on the action potential profile of 21S cells

The experiments reported in Fig. 3 were performed using the same protocol as in Fig. 1F. In the presence of 2 μM WAY (Fig. 3B), the action potential upstroke and the initial rapid repolarization were unaffected; however, the subsequent slow repolarization was completely abolished. The addition of TTX on top (Fig. 3D) evidently impaired any electrical activity of the cell, revealing the pure profile of the injected currents. In order to clarify whether the initial rapid repolarization of the action potential was due to the activation of the small I_{KDR} available in 21S cells, we used 20 mM TEA, a concentration that blocks this current completely and no more than 70% of I_{HERG} [11]. As shown in Fig. 3E, the initial rapid repolarization was in fact abolished by TEA.

On the whole, these results demonstrate that the contribution of I_{KDR} to the 21S cell action potential is limited to the very start of the repolarization phase, while it does not influence the long-lasting process of restoration of V_{REST}. This process is entirely sustained by I_{HERG}.

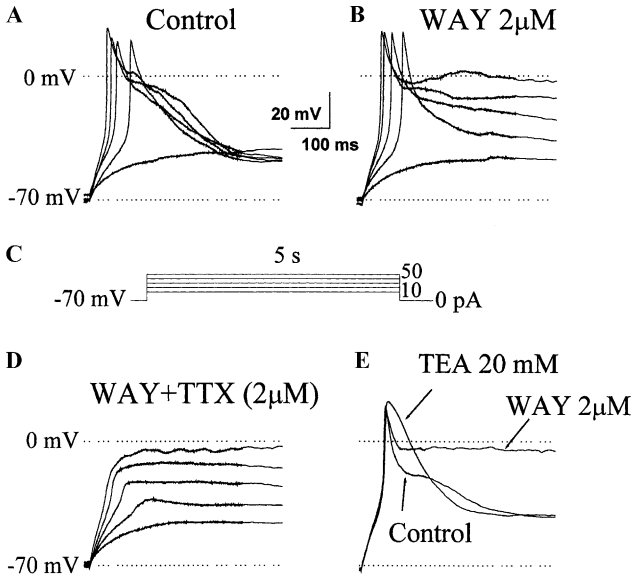

Fig. 3. The response of 21S cell action potential to currents inhibitors. (A–D) A typical 21S cell was stimulated, using the protocol reported in (C), and exposed to 2 μM WAY (B), or WAY + TTX (2 μM) (D); (E) traces obtained from one typical S cell injected with 50 pA currents under the following conditions: standard external solution (control), 20 mM TEA and, after washing, 2 μM WAY.

The double physiological role of I_{HERG} in 21S cells

To simultaneously estimate the role of I_{HERG} in 21S cell V_{REST} and action potential, we used the perforated patch-clamp technique that allows a long-lasting maintenance of cells at their spontaneous V_{REST}. In these experiments, the action potentials were elicited by very brief depolarizing stimuli, so that practically the entire action potential could develop after the injected currents were switched off (see protocol in Fig. 4C).

In Figs. 4A and B is reported the time-course of the membrane potential continuously recorded in current-clamp from two typical 21S cells initially endowed with a V_{REST} of −42 and −53 mV, respectively. At various times, short pulses of positive currents of increasing amplitude were applied (corresponding to the vertical deflections in the diagrams). When the cells were perfused with 2 μM WAY, they underwent a profound depolarization that reverted after the inhibitor was removed. This demonstrates that in 21S cells V_{REST} is governed by I_{HERG}, in keeping with the feature of the window conductance of this current (see Fig. 2J). Still under WAY perfusion, the cells were repolarized by manual injection of currents suitable to reset the original V_{REST} and again stimulated by applying depolarizing currents. By this procedure we obtained recordings either in the absence or in the presence of WAY. This allowed an estimate of the contribution of I_{HERG} to the action potential profile. This contribution emerges from Fig. 4D, where traces taken from Fig. 4A, representing the repolarization phase either in the absence or in the presence of 2 μM WAY, and after washing out the inhibitor, are superimposed. It is here evident that, not only WAY retarded the repolarization kinetics of the action potential, but also abolished the after-hyperpolarization, displayed in the control. This hyperpolarization was restored upon WAY washing out (square symbols).

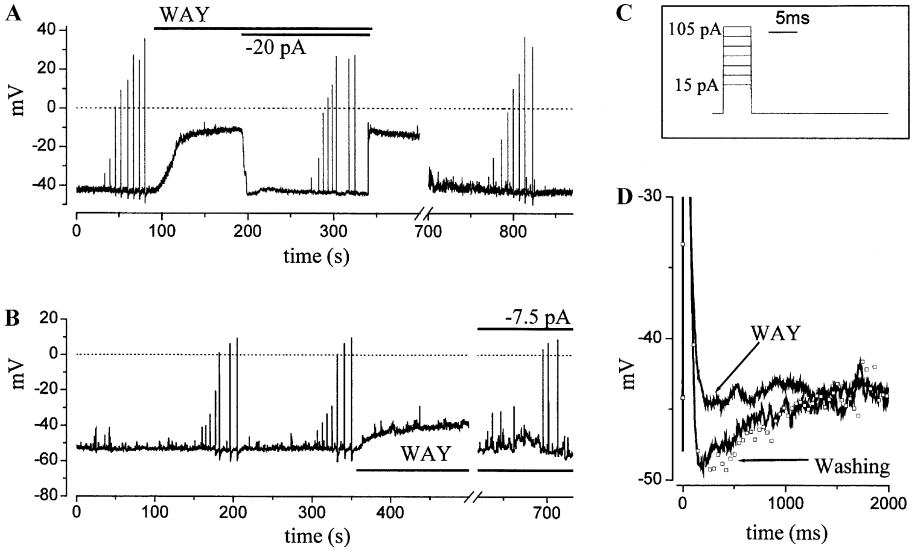

Fig. 4. The electrical activity of 21S cells measured in perforated patch-clamp experiments (see Materials and methods). Records obtained with the protocol reported in (C). (A,B) Effects of 2 μM WAY on V_{REST} and on action potential of 21S cells. During exposure to WAY, the cells in (A) and (B) were repolarized by manual injection of −20 or −7.5 pA, respectively, in order to reset the original resting (−42 and −53 mV, respectively). Vertical deflections correspond to the voltage responses to the stimulating current injections; (D) superimposed recordings taken from (A), showing the effects of 2 μM WAY on the after-hyperpolarization of action potential. Traces refer to the 90 pA injected current. Square symbols represent recovery after washing out of WAY with standard external solution.

On the whole, these results demonstrate that: (i) V_{REST} of 21S cells is governed by I_{HERG}, so that the inhibition of this current produces the cell depolarization; (ii) at potential held at V_{REST}, 21S cells respond to depolarizing stimuli with overshooting action potentials followed by an after-hyperpolarization; (iii) the bulk of the repolarization phase and the after-hyperpolarization are sustained by I_{HERG}. This double role of I_{HERG} and the kind of its modulation profoundly affect the electrophysiology of S cells. In fact, the voltage dependent features of this current (slow activation in depolarization and fast inactivation in hyperpolarization) not only limit the membrane polarization at rest, but also account for the unusual length of the action potential repolarization phase. The association of this peculiar excitable profile to a glial-oriented phenotype raises unsolved questions, as to the role of these S cells in the complex cellular interplay underlying the neural crest progenitor's differentiation and its malignant alterations leading to neuroblastoma [20]. So far, the long-lasting shape of their action potential may be envisaged as a secretory signal producing neurotrophic factors to be utilized by the S cells themselves or by the neuron-type cells in autocrinuous or paracrinous circuits [21]. Such factors are normally secreted by glial and neuronal cells in their reciprocal supportive interactions underlying the development of the nervous system [21,22].

Consistently, an electrophysiological profile in some respects similar to that here shown for 21S cells has been reported for astrocytes during CNS development; these cells, in fact, express relatively high levels of Na^+ channels in combination with a very small I_{KDR} [23,24]. In these cases, however, I_{HERG} was never expressed.

In conclusion, the 21S-type cells emerged from our study as a cellular compartment of the adrenergic SY5Y clone, endowed with electrophysiological features that are both hitherto unknown and liable to mark a specific differentiation pattern of neural crest progenitors.

Acknowledgments

The skillful technical support of Marco Cutrì is gratefully acknowledged. This work was supported by grants from the Associazione Italiana per la Ricerca sul Cancro (AIRC), Ministero dell'Università e della Ricerca Scientifica e Tecnologica (MURST, COFIN 2000-01), Project 1046 of Comitato Promotore Telethon and MURST-COFIN No. 9705157384 to E.W., Associazione Italiana contro le Leucemie (AIL) Firenze, and Ente Cassa di Risparmio di Firenze (CARIFI).

References

[1] M.C. Sanguinetti, C. Jiang, M.E. Curran, M.T. Keating, A mechanistic link between an inherited and an acquired cardiac arrhythmia: HERG encodes the IKr potassium channel, Cell. Apr. 21 81 (2) (1995) 299–307.

[2] C.K. Bauer, J.R. Schwarz, Physiology of EAG K^+ channels, J. Membr. Biol. 182 (2001) 1–15.

[3] A. Arcangeli, B. Rosati, A. Cherubini, C. Ziller, O. Crociani, L. Fontana, E. Wanke, M. Olivotto, HERG and IRK-like inward rectifier currents are sequentially expressed during neuronal development of neural crest cells and their derivates, Eur. J. Neurosci. 9 (1997) 2596–2604.

[4] L. Bianchi, B. Wible, A. Arcangeli, M. Taglialatela, F. Morra, P. Castaldo, O. Crociani, B. Rosati, L. Faravelli, M. Olivotto, E. Wanke, *herg* encodes a K^+ current highly conserved in tumors of different histogenesis: a selective advantage for cancer cells? Cancer Res. 58 (1998) 815–822.

[5] J.I. Vandenberg, B.D. Walker, T.J. Campbell, HERG K^+ channels: friend and foe, Trends Pharmacol. Sci. 22 (2001) 240–246.

[6] N. Chiesa, B. Rosati, A. Arcangeli, M. Olivotto, E. Wanke, A novel role of HERG K^+ channels: spike-frequency adaptation, J. Physiol. 501.2 (1997) 313–318.

[7] V. Ciccarone, B.A. Spengler, M.B. Meyers, J.L. Biedler, R.A. Ross, Phenotypic diversification in human neuroblastoma cells: expression of distinct neural crest lineages, Cancer Res. 49 (1989) 219–225.

[8] S.V. Gaitonde, W. Qi, R.R. Falsey, N. Sidell, J.D. Martinez, Morphological conversion of a neuroblastoma-derived cell line by E6-mediated p53 degradation, Cell Growth Differ. 12 (2001) 19–27.

[9] A. Arcangeli, L. Bianchi, A. Becchetti, C. Faravelli, M. Coronello, E. Mini, M. Olivotto, E. Wanke, A novel inward-rectifying K^+ with a cells cycle dependence governs the resting potential of mammalian neuroblastoma cells, J. Physiol. (Lond.) 489 (1995) 455–471.

[10] O.P. Hamil, A. Marty, E. Neher, F. Sakmann, F.J. Sigworth, Improved patch-clamp techniques for high resolution current recording from cells and cell-free membrane patches, Pflugers Arch. 391 (1981) 85–100.

[11] L. Faravelli, A. Arcangeli, M. Olivotto, E. Wanke, A HERG-like channel in rat F-11 DRG cell line: pharmacological identification and biophysical characterization, J. Physiol. 496 (1996) 13–23.

[12] P.L. Smith, T. Baukrowitz, G. Yellen, The inward rectification mechanism of the HERG cardiac potassium channel, Nature 379 (1996) 833–836.

[13] J. Rae, K. Cooper, E. Gates, M. Watsky, Low access resistance perforated patch recordings using amphotericin B, J. Neurosci. Meth. 37 (1991) 15–26.

[14] W.J. Rettig, B.A. Spengler, P.G. Chesa, L.J. Old, J.L. Biedler, Coordinate changes in neuronal phenotype and surface antigen expression in human neuroblastoma cells variants, Cancer Res. 47 (1987) 1383–1389.

[15] M. Toselli, P. Tosetti, V. Taglietti, Functional changes in sodium conductance in the human neuroblastoma cell line SH-SY5Y during in vitro differentiation, J. Neurophysiol. 76 (1996) 3920–3927.

[16] P. Tosetti, V. Taglietti, M. Toselli, Functional changes in potassium conductance in the human neuroblastoma cell line SH-SY5Y during in vitro differentiation, J. Neurophysiol. 79 (1998) 648–658.

[17] A. Bordey, H. Sontheimer, Electrophysiological properties of human astrocytic tumor cells in situ: Enigma of spiking glial cells, J. Neurophysiol. 79 (1998) 2782–2793.

[18] R. Meyer, S.H. Heinemann, Characterization of an eag-like potassium channel in human neuroblastoma cells, J. Physiol. 508 (1998) 46–49.

[19] M. Toselli, S. Masetto, P. Rossi, V. Taglietti, Characterization of voltage independent calcium current in the human neuroblastoma cell line SH-SY5Y during differentiation, Eur. J. Neurosci. 3 (1991) 514–522.

[20] J.L. Biedler, B.A. Spengler, C. Tien-Ding, R.A. Ross, Transdifferentiation of human neuroblastoma cells results in coordinate loss of neuronal and malignant properties, Prog. Clin. Biol. Res. 271 (1988) 265–276.
[21] L.A. Casulari, R.C. Melcangi, F. Piva, L. Martini, R. Maggi, Factors released by rat type 1 astrocytes exert different effects on the proliferation of human neuroblastoma cells (SH-SY5Y) in vitro, Endocr.-Rel. Cancer 7 (2000) 63–71.
[22] M.L. Reynolds, C.J. Woolf, Reciprocal Schwann cell–axon interactions, Curr. Opin. Neurobiol. 3 (1993) 683–693.
[23] E.R.O. Connor, H. Sontheimer, D.D. Spencer, N. De Lanerolle, Astrocytes from human hippocampal epileptogenic foci exhibit action potential-like responses, Epilepsia 39 (4) (1998) 347–354.
[24] A. Gritti, B. Rosati, M. Lecchi, A.L. Vescovi, E. Wanke, Excitable properties in astrocytes derived from human embryonic CNS stem cells, Eur. J. Neurosci. 12 (2000) 3549–3559.